Tissue Evidence of the Testosterone Role on the Abnormal Growth and Aging Effects Reversion in the Gerbil (*Meriones unguiculatus*) Prostate

WELLERSON RODRIGO SCARANO,[1] PATRICIA SIMONE LEITE VILAMAIOR,[2] AND SEBASTIÃO ROBERTO TABOGA[3]*

[1]Cell Biology Department, Biology Institute, UNICAMP, Campinas, São Paulo, Brazil
[2]Rio Preto Universitary Center, UNIRP, Biological Sciences School, São José do Rio Preto, São Paulo, Brazil
[3]Microscopy and Microanalysis Laboratory, Department of Biology, IBILCE, São Paulo State University, São José do Rio Preto, São Paulo, Brazil

ABSTRACT

Prostate differentiation during embryogenesis and its further homeostatic state maintenance during adult life depend on androgens. Abundant biological data suggest that androgens play an important role in the development of the prostate cancer and other prostatic diseases. The objective of this work was to evaluate the effects of the testosterone supplementation in gerbil (a new experimental model) at different ages. Tissues from experimental animals were studied by histological and histochemistry procedures, androgen receptor immunohistochemistry assay, morphometric-stereological analysis, and transmission electron microscopy (TEM). After the treatment were observed increase of prostate weight and epithelium height in all ages studied. In some adult and aged treated animals, hyperplasic and displasic process were observed, including prostatic intraepithelial neoplasias and adenocarcinomas. Increase of the thickness of the smooth muscle cell (SMC) layer was observed in pubescent and adult animals and TEM revealed apparent SMC hypertrophy. An apparent increase in the frequency of blood vessels distributed by the subepithelial stroma in the treated animals was noticed. Reversion of the natural effects of aging on the prostate was observed in the aged treated animals in some acini of the gland. These data demonstrate that the gerbil prostate is susceptible to androgenic action at the studied ages and it can serve, for example, as experimental model to studies of prostate neoplasic process induction and hormonal therapy in aged animals. Anat Rec Part A, 288A:1190–1200, 2006.

Key words: testosterone; prostate; stroma; epithelium; gerbil

Androgens are steroid hormones that induce the differentiation and maturation of the male reproductive organs and the development of the male secondary sex characteristics. Prostate differentiation during embryogenesis and its further homeostatic state maintenance during adult life depend on androgens. The normal prostatic epithelium is composed of different cells types that have varying androgen sensitivities, including androgen-independent basal stem cells, androgen-dependent luminal secretory cells, and androgen-independent but androgen-sensitive

Grant sponsor: State of São Paulo Research Foundation (FAPESP); Grant number: 02/12942-6.

*Correspondence to: Sebatião Roberto Taboga, IBILCE, UNESP, Departamento de Biologia, Rua Cristóvão Colombo, 2265, Jardim Nazareth, São José do Rio Preto, SP, Brazil. Fax: 55-17-32212390. E-mail: taboga@ibilce.unesp.br

Received 25 May 2006; Accepted 9 August 2006
DOI 10.1002/ar.a.20391
Published online 9 October 2006 in Wiley InterScience (www.interscience.wiley.com).

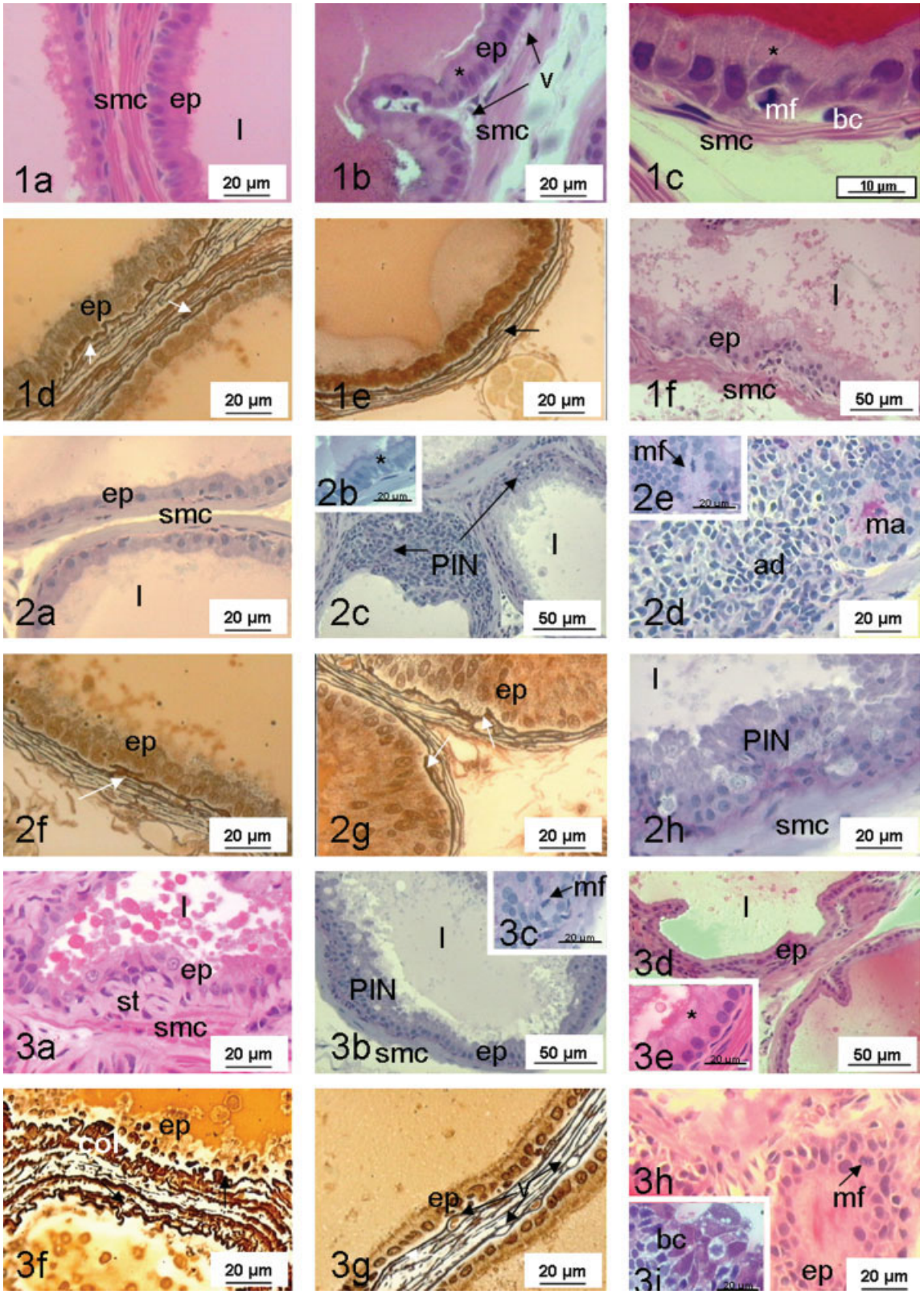

Figures 1–3 (See overleaf.).

transitional cells (Isaacs, 1999). Thus, the normal prostate is inherently heterogeneous in its sensitivity to androgens.

Testosterone enters the prostate cell by passive or active diffusion. Once in the cytoplasm, it will remain as testosterone or transform to DHT by 5α-reductase and will be attached predominantly to a cytoplasmic receptor or androgen receptor (AR) or to a nuclear receptor (Rosner et al., 1999).

Epithelial ARs are required for expression of AR-dependent prostatic secretory proteins but many androgenic effects on epithelium, as regulation of proliferation of normal epithelia, are elicited by paracrine factors produced by AR-positive stroma (Donjacour and Cunha, 1993). Conversely, hormonal regulation of epithelial differentiation and functions requires direct hormonal action-mediated epithelial hormone receptors (Buchanan et al., 1998, 1999). Androgenic regulation of prostatic epithelial cells during malignant transformation of prostatic epithelial cells appears to involve conversion from a paracrine to an autocrine mechanism of androgen-stimulated growth (Gao et al., 2001).

Abundant biological data suggest that androgens play an important role in the development of the prostate cancer. The growth and maintenance of the prostate are dependent on androgens, prostate cancer regresses after androgen ablation or antiandrogen therapy, and testosterone induces prostate tumors in laboratory animals (Shirai et al., 2000; So et al., 2003; Zanetoni et al., 2005).

Current evidence indicates that serum levels of sex hormones carry no relations to the development of prostate cancer, and there is either no change or only a modest increase in prostate specific antigen (PSA) after testosterone administration (Nomura et al., 1988). The suspicion of prostate cancer is, however, an absolute contraindication for androgen therapy.

On the basis of these considerations, the aim of the present study was to investigate the effects of testosterone supplementation on the gerbil's prostate at different phases of the postnatal development, trying to establish the possible model to experimental carcinogenesis. In addition, the Mongolian gerbil (*Meriones unguiculatus*) has been recognized in some biomedical sciences, such as immunology (Nawa et al., 1994), physiology (Nolan et al., 1990), and morphology (Custódio et al., 2004; Pinheiro et al., 2003; Santos et al., 2003, 2006; Corradi et al., 2004). More recently, gerbil has also been suggested as a suitable model for studies on mammalian aging (Pegorin de Campos et al., 2006). Gerbil's prostate has compact lobes, somewhat similar to the human prostate, unlike rats and mice, which have distinct lobes (Pinheiro et al., 2003; Góes et al., 2006). Previous data from our laboratory has demonstrated that histological, histochemical, and ultrastructural features of the adult gerbil's prostate are comparable to the human prostate. Besides, we have observed that old gerbils (12 months) may spontaneously develop benign prostate hyperplasia, cancer, and other prostate disorders (Pegorin de Campos et al., 2006).

MATERIALS AND METHODS

Animals and Hormone Treatments

To accomplish the work, 30 male *Meriones unguiculatus* gerbils of the following ages were used: pubescent (40 days after birth), adult (120 days after birth), and aged (12 months after birth).

For each age group, the animals were divided in two groups of five each for control and treated groups. In each case, the treated group received in alternate days subcutaneous injections of testosterone cipionate diluted in vegetal oil (10 mg/ml) at a dose of 0.1 ml/application/animal (1 mg/application) for 21 days, while the control group received only vegetal oil (Santos et al., 2006).

After 21 days of treatment, the animals of all ages and of both groups were anesthetized lightly by CO_2 inhalation and killed by cervical displacement. After this procedure, the animals were weighed and immediately decapitated to blood collecting. The ventral prostate was removed, weighed, and immediately submitted to light microscopy and ultrastructural procedures.

Animal handling and experiments were done according to the ethical guidelines of the São Paulo State University following the Guide for Care and Use of Laboratory Animals. The number of individuals employed in this work was justified by the large number of analytical procedures employed.

Hormonal Serum Levels

Circulating plasma testosterone levels were determined by immunochemical assays. Blood was collected and the serum was separated by centrifugation and stored at −20°C for subsequent hormone assay. The determination of serum levels of testosterone was performed by luminescence immunoassay (mouse antibodies antitestosterone; Johnson and Johnson) in automatic analyzer from Vitros-ECi-Johnson and Johnson for ultrasensitive chemiluminescence detection. The intra-assay and interassay variation was 4.6% and 4.3%, respectively.

Fig. 1–3. Fig. 1. Histological sections from pubescent animals: H&E (**a**–**c** and **f**); reticulin (**d** and **e**). Control animals: a and d; testosterone-treated animals: b, c, e, and f. a shows the general tissue aspect. In b, the arrows point to the blood vessels (v) in the stroma, and a clear supranuclear area is evident (asterisk). In c occur the presence of mitotic figures (fm), basal cells (bc), and prominent Golgi area (asterisk). In d and e, the arrows point to reticular fibers of the stroma. f shows the displasic secretory epithelium. l, lumen; ep, epithelium. Fig. 2. Histological sections from adult animals: H&E (**a**–**e** and **h**); reticulin (**f** and **g**). Control animals: a and f; testosterone-treated group: b, c, d, e, g, and h. a: General tissue aspect. In b, prominent supranuclear area (asterisk) of the nonaltered epithelium. c shows high grade and low grade of the PIN. In d, adenocarcinoma (ad) and presence of microacini (ma) surrounded by tumorous cells are observed. e: Detail of the carcinoma showing division of cells (mf). f and g: Arrows point to reticular fibers of the stroma. In h, presence of the PIN and some nuclei of the cells with a differentiated chromatin distribution pattern. Fig. 3. Histological sections from aged animals: H&E (**a**–**e**, **h**, and **i**); reticulin (**f** and **g**). Control animals: a and f; testosterone-treated group: b, c, d, e, g, h, and i. a: General aspect of the tissue where it is observed a displasic secretory epithelium. The prominent subepithelial stroma (st) and folds in the basal membrane. In b, a focal PIN and high epithelium. c: Detail of a PIN cell in division (mf, mitotic figure). d and e: A high secretory epithelium and prominence of the supranuclear clear area (asterisk). f and g: Arrows point to reticular fibers of the stroma. In f, collagen fibers (col) are abundant in subepithelial stroma, and in g, the evident presence of the blood vessels (v). h: Hiperplasic process in some microacini with mitotic figures. In i, presence of the basophilic cells of granular cytoplasmic aspect (bc).

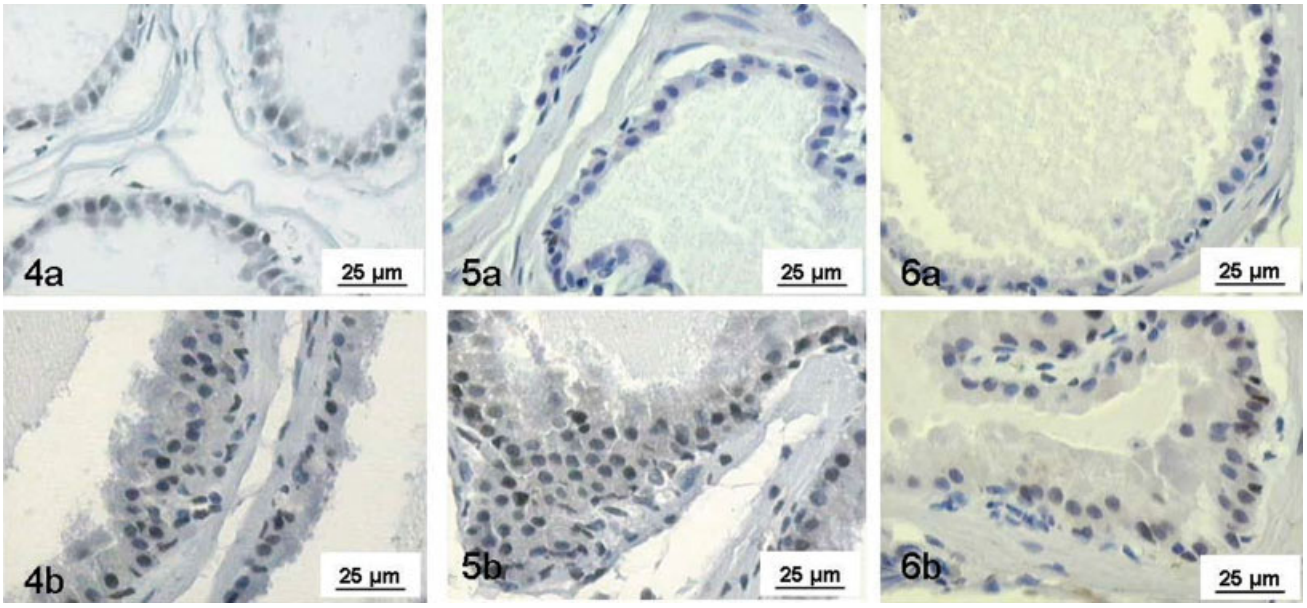

Fig. 4–6. Fig. 4. AR immunohistochemistry. Pubescent animals: **a** (control) and **b** (treated). Fig. 5. AR immunohistochemistry. Adult animals: **a** (control) and **b** (treated). Fig. 6. AR immunohistochemistry. Aged animals: **a** (control) and **b** (treated).

Histochemistry

Ventral prostates of control and testosterone-treated groups were cut into fragments and immediately fixed by immersion for 24 hr in Karnovsky's fixative (0.1 M Sörensën phosphate buffer, pH 7.2, containing 5% paraformaldehyde and 2.5% glutaraldehyde). Fixed tissue samples were dehydrated in a graded ethanol series and embedded in glycol methacrylate resin (Leica historesin embedding kit) and part of prostate fragments was embedded in paraplast for immunohistochemical tests. Histological sections (3 µm) were subjected to hematoxylin-eosin (H&E) staining for general studies, to Gömöri's reticulin (Gömöri, 1937) staining for collagen and reticular fibers and to Feulgen (Mello and Vidal, 1980) staining for nuclear study. Microscopic analyses were performed on Zeiss-Jenaval or Olympus photomicroscopes, and the microscopic fields were digitalized using the Image-Pro Plus version 4.5 for Windows software.

Morphometric and Stereological Analysis

Using an analyzing system of images (Image Pro-Plus), H&E and Feulgen sections were analyzed. Images of 50 histological fields for each experimental group in the ages studied were analyzed, such that histological fragments of all animals were evaluated equally. The morphometric analyze was performed to evaluate epithelium height, smooth muscle cell layer thickness, and nuclear area of the secretory epithelial cells. For this comparative study, 200 measurements to each parameter were realized. Stereologic analyses were obtained by Weibel's multipurpose graticulate with 120 points and 60 test lines (Weibel, 1979) to compare the relative proportion (volume density) among the prostatic components (epithelium, stroma, and lumen of acinus) in the different ages in both experimental groups. The volume (or absolute volume) of each of these compartments was determined by multiplying the volume density by the mean prostatic weight based on the determination that 1 mg of fresh rat ventral tissue had a volume of approximately 1 mm^3 according Vilamaior et al. (2006).

Statistical Analysis

The testosterone effects on gerbil ventral prostate were evaluated by analyses of mean ± standard deviation (SD) of several parameters such as epithelium height, smooth muscle cell thickness, nuclear perimeter, nuclear area, relative and absolute proportions of prostatic tissue compartments. Statistical analysis was performed in the Statistica 6.0 software (StatSoft). The hypothesis test Anova and Tukey's honest significant difference (HSD) test were employed, and $P \leq 0.05$ was considered statistically significant.

Transmission Electron Microscopy

The ventral prostates of control and treated gerbils were processed for transmission electron microscopy as described previously (De Carvalho et al., 1994), employing the fixation procedure of Cotta-Pereira et al. (1976). Briefly, tissue fragments were fixed in 0.25% tannic acid plus 3% glutaraldehyde in Millonig's buffer, dehydrated in acetone, and embedded in Araldite resin. Ultrathin sections (50–75 nm) obtained with a diamond knife were stained by uranyl acetate and lead citrate. Observation and electron micrographs were made with a LEO-Zeiss 906 transmission electron microscope.

Immunohistochemistry (IHC)

AR (N-20; 1:100 dilution; rabbit polyclonal antibody; Santa Cruz Biotechonology, Santa Cruz, CA) was used for IHC. Immunohistochemistry staining was performed using

the avidin-biotin complex (ABC) kit (Santa Cruz Biotechnology). The paraplast-embedded sections (5 μm) were dewaxed and then rehydrated in graded alcohol and distilled water. Antigenic recuperation was realized in citrate buffer in high temperature (100°C) for 45 min. Endogenous peroxidase activity was blocked with 0.3% hydrogen peroxide in methanol for 45 min, followed by a quick rinse in distilled water and phosphate-buffered saline (PBS). Sections were incubated with normal goat and primary antibody at 4°C overnight. The slides were then incubated with the biotinylated antirabbit at 37°C followed by peroxidase-conjugated ABCs and diaminobenzidine (DAB). The sections were then counterstained with hematoxylin of Harris. For negative control, the primary antibody was replaced with the corresponding normal isotype serum.

RESULTS

The prostate gland in intact animals presented acini with simple cylindrical epithelium, surrounded by a fine strip of vascularized conjunctive tissue and a layer of smooth muscle cells (SMCs; Figs. 1a, 2a, and 3a). Among the acini, loose vascularized conjunctive tissue was observed.

The epithelial cells of the gland have evident secretory characteristics and in some places extrusion granules could be observed, typical of apocrine secretory cells (Figs. 1a and 3a). Other secretory characteristics were based on the presence of clear supranuclear areas designated to be the area of the Golgi apparatus (1a, 2a and 3a). Dysplasic regions were observed in aged control animals in some acini (Fig. 3a).

Ultrastructurally, the secretory glandular epithelium was formed by prismatic cells that vary from short to high, depending on the age, whereas the nucleus had basal polarity and a large amount of endoplasmic reticulum (Figs. 7 and 8). Besides, it was possible to differentiate clearly between the secretor cells and the basal cells (Fig. 7). The basal cells were located at the base of the epithelium in intimate contact with the basal lamina and they were poor in endoplasmic reticulum (Fig. 7). Sometimes it was possible to identify electrondenses corpuscles, probably of ceramide bodies, between the epithelial cells (Fig. 7).

Adjacent to the epithelium and intermixed among the smooth muscle cells were observed collagen and reticular fibers (Fig. 9). However, the reticular fibers became denser at the epithelial base, adjacent to the basal membrane and intermixed among the SMCs (Figs. 1d, 2f, and 3f). In the aged animals, there was a stromal rearrangement, where accumulation of collagen fibrils was observed adjacent to the epithelium and among the prostatic acini (Figs. 3f, 10, and 11), and apparent hypertrophy of the SMCs (Fig. 10), as can be observed in Table 1, which compares the control animals of the other ages in relation to the thickness of the SMC layer and to the relative volume occupied by the stromal compartment. Besides, there was decrease in the serum testosterone levels in the aged group in relation to the pubescent and adult animals (Fig. 20).

The testosterone-treated group presented significant increase in the weight of the prostate, but without suffering variation in the corporal weight when compared to the control groups (Table 1). Increase was observed in the height of the secretor epithelium in relation to the control group at all the ages (Figs. 1b and c, 2b, 3e, and 12, Table 1), as well as in the volume occupied by the epithelium at the pubescent and adult ages. After treatment with testosterone, the nuclear area and perimeter were unaltered only in the pubescent animals, while in the adult and aged animals there were increases of the nuclear area and perimeter in the treated animals (Table 1).

The morphometric data indicated significant increase in the thickness of the SMC layer of the acini in relation to the control group at the pubescent and adult ages, while in the aged animals there was a decrease in the treated animals. In the stroma, there was no alteration in relation to the relative volume among the groups in the pubescent and adult animals, with a decrease only in the treated aged animals (Table 1). The absolute data showed significant increases in all of the appraised parameters since there was increase of the prostatic weight without alteration in the body weight (Table 1).

The histopathological analysis showed that in the testosterone-treated animals at all ages occurred an increase in the supranuclear area, where they concentrate in the synthesis organelles, mainly the Golgi apparatus, which appears prominent and dilated after the treatment (Figs. 1b and c, 2b, 3e, 12, 13, and 15).

An enlargement of the endoplasmic reticulum cisterns was noticed, mainly in the treated adult animals, which appeared with a vesiculous aspect, in all cytoplasm of the secretory cells (Fig. 14).

Mitotic figures were evidenced at all ages after the testosterone treatment (Figs. 1c, 2e, and 3c). In the pubescent animals, this treatment did not provoke relevant alterations, but dysplasias in some acini were observed (Fig. 1f). In the adult animals, different degrees of prostatic intraepithelial neoplasia (PIN) as high-grade PIN (Fig. 2c) and low-grade PIN (Fig. 2h) were observed. In general, our understanding of PIN in Mongolian gerbil prostate is based on the microscopic grading of PIN performed to human prostate according the architectural pattern of epithelium atypia or dysplasia and nuclear pleomorphism of epithelial cells (Taboga et al., 2003); the increase of the PIN gradation is correlated with the increase of parameters described above. Besides, some of these animals presented adenocarcinomas and presence of microacini surrounded by tumorous cells (Figs. 2d and e). In some areas of PIN, some nuclei were observed with a differentiated chromatin distribution pattern (Fig. 2h).

In the aged individuals, the treatment with testosterone evidenced two different effects: in some acini, reversal of the aging process was observed, where there were noticed increase of the epithelium, decrease of fibrillar elements of the extracellular matrix, decrease in the thickness of SMC layer, and increase in the relative volume of the lumen (Figs. 3d and e and 18, Table 1), each resembling, phenotypically, the adult control animals (Fig. 2a); in other acini, hyperplasic processes and presence of PIN were evidenced (Fig. 3b, c, and h), as well as the presence of cells denominated here as basophiles of granular cytoplasmic aspect (Fig. 3i).

An apparent increase in the frequency of blood vessels distributed by the subepithelial stroma in the treated animals was noticed (Figs. 1b, 3g, and 19). In the stromal compartment of the treated pubescent animals, some populations of SMCs appeared hypertrophic, but without clear cytoplasmic alterations (Fig. 17). In treated adult animals, it was common to observe hypertrophic cells with prominent nucleoli and abundant endoplasmic reticulum (Fig. 16). In general, alterations in the distribution

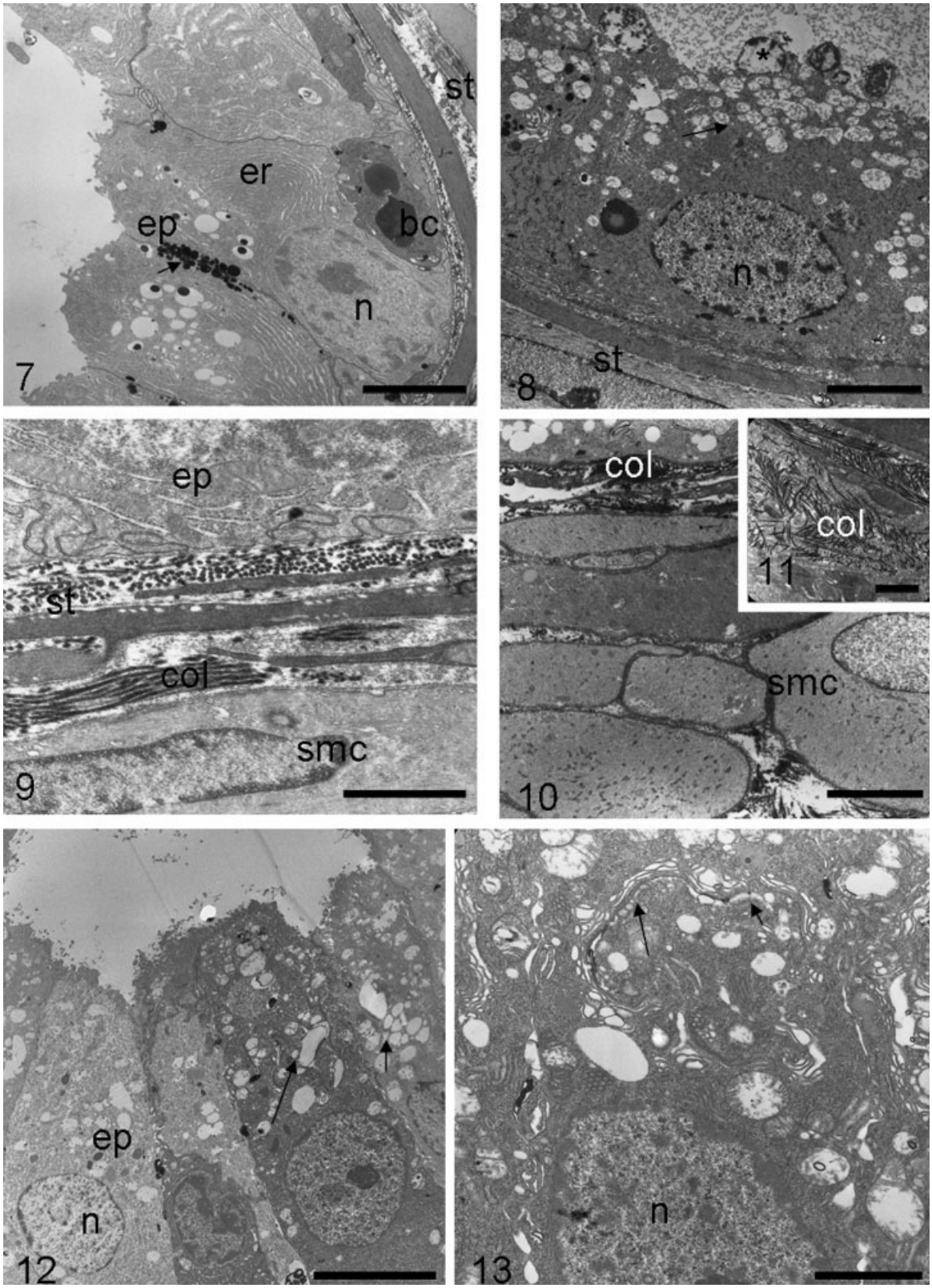

Figures 7–13 (See overleaf.).

TABLE 1. Quantitative exploratory analysis from experimental animals at different ages

	Experimental Groups					
	Pubescent gerbil		Adult gerbil		Aged gerbil	
Quantitative data	Control	Testosterone	Control	Testosterone	Control	Testosterone
Morphometry (μm)						
Epithelium height	17.18 ± 3.66	23.90* ± 8.10	9.08 ± 2.14	17.81* ± 4.18	10.89 ± 2.21	14.69* ± 2.29
SMC layer thickness	8.10 ± 3.08	10.49* ± 3.20	8.51 ± 1.85	10.61* ± 2.44	14.64 ± 5.10	11.39* ± 2.95
Karyometry of secretory cells						
Nuclear area (μm^2)	29.86 ± 7.57	29.38 ± 5.49	23.15 ± 3.84	30.90* ± 6.46	19.81 ± 4.06	29.95* ± 5.70
Nuclear perimeter (μm)	22.30 ± 3.48	22.26 ± 2.90	21.27 ± 2.80	23.25* ± 3.61	19.78 ± 3.75	22.86* ± 3.22
Relative proportion of tissue components (%) – Volume density						
Epithelium	16.50 ± 2.21	21.77* ± 2.21	17.34 ± 2.64	22.04* ± 2.26	19.08 ± 3.14	18.65 ± 2.52
Stroma	42.42 ± 7.91	42.35 ± 5.82	38.77 ± 10.04	41.77 ± 7.16	45.73 ± 7.00	35.73* ± 8.80
Lumen	41.08 ± 7.51	35.88* ± 5.04	43.89 ± 10.52	36.19* ± 6.14	35.19 ± 5.87	45.62* ± 9.27
Absolute proportion of tissue components (mg) – Absolute volume						
Epithelium	0.12 ± 0.02	0.21* ± 0.02	0.18 ± 0.03	0.34* ± 0.04	0.09 ± 0.01	0.23* ± 0.03
Stroma	0.30 ± 0.06	0.41* ± 0.06	0.41 ± 0.11	0.66* ± 0.11	0.21 ± 0.03	0.44* ± 0.11
Lumen	0.29 ± 0.05	0.34* ± 0.15	0.46 ± 0.11	0.57* ± 0.10	0.17 ± 0.03	0.56* ± 0.11
Body weight (mg)	62.24 ± 5.82	61.92 ± 6.95	80.02 ± 8.77	79.42 ± 6.78	67.02 ± 7.51	77.62 ± 5.67
Prostate weight (mg)	0.71 ± 0.06	0.96* ± 0.12	1.05 ± 0.04	1.57* ± 0.38	0.47 ± 0.19	1.22* ± 0.17
Relative prostate weight (mg prostate/ mg body weight)	0.011 ± 0.002	0.016* ± 0.003	0.013 ± 0.001	0.193* ± 0.004	0.007 ± 0.003	0.016* ± 0.003

Values represent mean ± SD. Statistical analysis based on the Anova and Tukey Tests.
*Significant ($P \leq 0.05$) vs. control group.

and density of collagen and reticular fibers were not observed under light microscopy, although in some areas rapid accumulation of collagen fibrils was observed by electronic microscopy when compared to the control group (Figs. 1e, 2g, 9, and 16).

In the aged animals, the testosterone treatment showed a pattern of stromal organization similar to that observed in untreated adult animals (Fig. 3g), differing from the pattern of the control group where abundance of components of the extracellular matrix was found (Fig. 3f).

The data also show that with the advancement of chronological age, the AR expression becomes less frequent, increasing the index of negative demarcation among the untreated animals (Figs. 4a, 5a, and 6a). After the treatment, at all of the ages, increase in the expression of the androgenic receptors was observed, mainly in the atypical regions, where the epithelium showed hyperplasic and dysplasic processes (Figs. 4–6).

DISCUSSION

The histology, histochemistry, and ultrastructure of the Mongolian gerbil prostate were described by Pegorin de Campos et al. (2006). The described aspects indicated that the prostate of this rodent seems to be a good model for experimental studies, because it is susceptible to pathological alterations similar to those found in the human prostate gland, besides being animals easy to maintain in captivity.

Androgens are required in functional activities and the normal growth of the prostate to maintain homeostasis of the organ (Cunha et al., 1986; Debes and Tindall, 2002). The functions of testosterone in the prostate are modulated by ARs, which control androgenic responses in the epithelium and in the stroma (Wang et al., 2001).

The increase in the weight of the organ after testosterone treatment is associated with the anabolic factor exerted by the testosterone, in which there is production of growth factors favoring prostatic hypertrophy (Thomson, 2001).

The increase of the epithelial height, along with the prominence of the Golgi area, demonstrates the probable increase in secretory activity of the epithelial cells in the treated animals in all the ages. Such association is directly related to an increase of the intracellular secretory machinery: rough endoplasmic reticulum (RER) and Golgi (Gross and Didio, 1987).

Fig. 7–13. Fig. 7. Ultrastructure figure. Pubescent control prostate. Detail of the epithelium (ep) and abundant endoplasmic reticulum cisternae (er). Presence of ceramides granules between the secretory epithelial cells (arrow). st, stroma; bc, basal cell; n, nuclei. Scale bar = 2.01 μm. Fig. 8. Ultrastructure figure. Adult control prostate. Epithelial cell with secretion vesicles (arrow) and blebs (apocrine secretion). n, nuclei; st, stroma. Scale bar = 2.01 μm. Fig. 9. Ultrastructure figure. Adult control prostate. Epithelium (ep)-stroma (st) transition. col, collagen fibers. Scale bar = 0.72 μm. Fig. 10. Ultrastructure figure. Aged control prostate showing the stromal compartment (st). Presence of bunches of collagen fibers in subepithelial stroma (col) and smooth muscle cells. Scale bar = 2.01 μm. Fig. 11. Ultrastructure figure. Aged control prostate. Subepithelial stroma with abundant collagen fibers. Scale bar = 0.56 μm. Fig. 12. Ultrastructure figure. Adult treated prostate. A high epithelium (ep) with dilated cisternae (arrow). n, nuclei. Scale bar = 4.34 μm. Fig. 13. Ultrastructure figure. Detail of the epithelial cell of adult treated prostate, where it is possible to observe a prominent Golgi (arrows). n, nuclei. Scale bar = 1.21 μm.

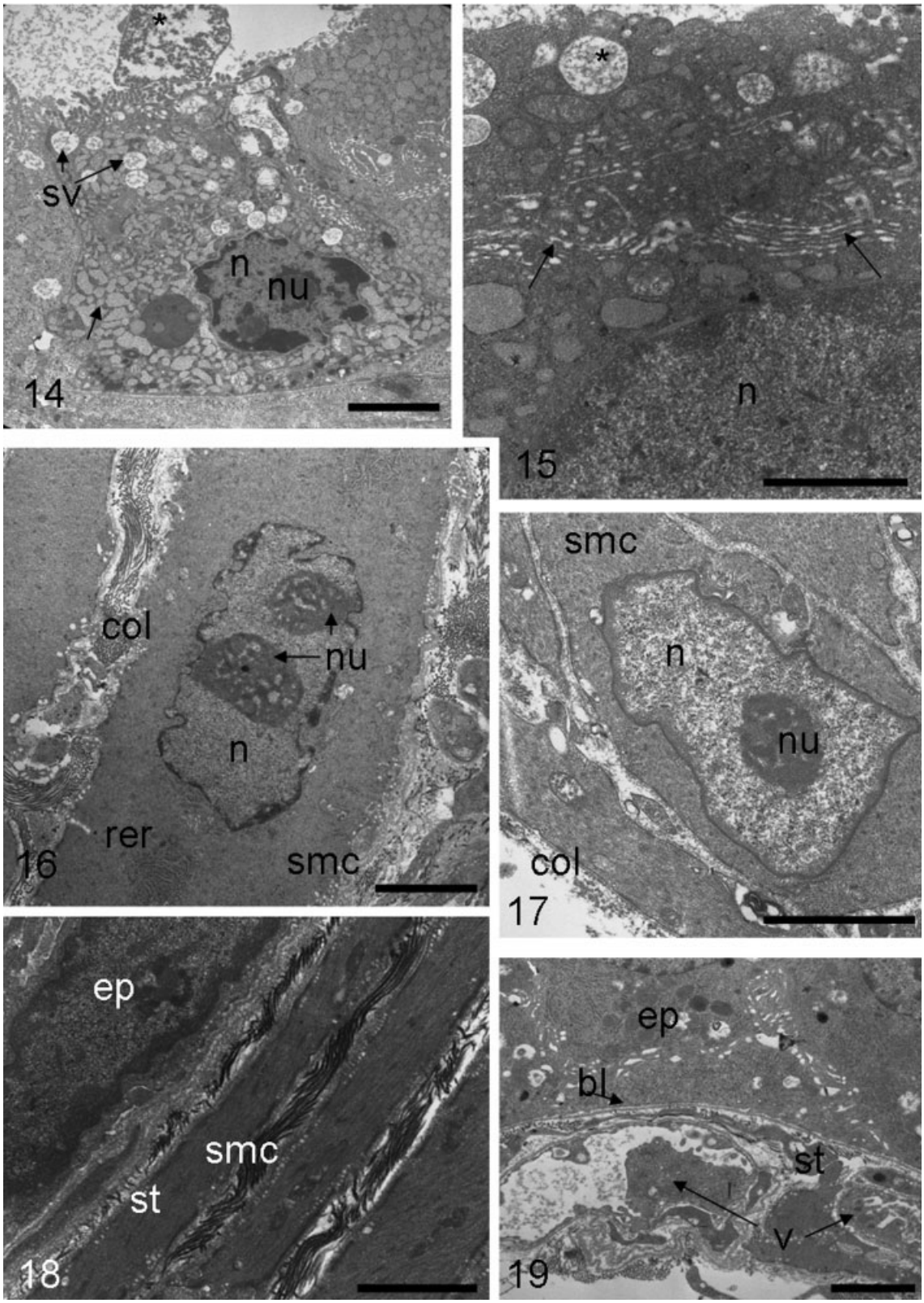

Figures 14–19 (See overleaf.).

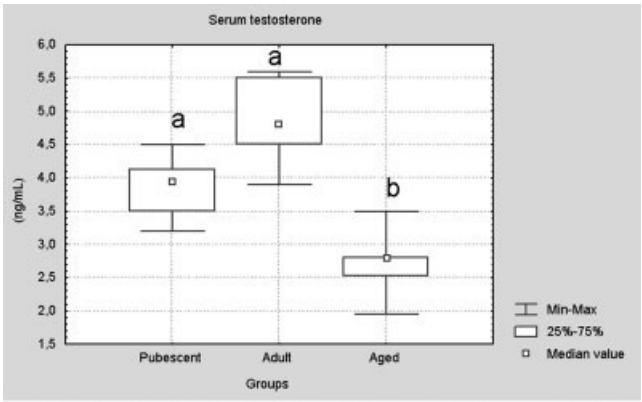

Fig. 20. Serum testosterone levels at the three ages studied.

The testosterone participates in the process of prostate development, including the secretory processes, stimulating the synthesis of constituent substances of the sperm (Price, 1963; Aumüller and Seitz, 1990; Rosai, 1996; Hayward et al., 1997; Thomson et al., 1997). Studies using castrated or aged animals with low androgenic levels show that testosterone is capable of increasing the height of epithelial cells and of the secretory apparatus (Scarano et al., 2003).

Heterogeneity was observed in the expression of ARs among the acini in all age groups. This fact is associated with the existence of cellular clones more sensitive to the androgenic stimulus and its effects. This justifies the presence of the acini with neoplasic lesions beside morphologically normal acini. In the treated groups, there was greater density of AR-positive cells, suggesting higher susceptibility to the androgenic action in these animals (Brandes, 1966). Besides, it was noticed that the cells of areas of PIN and focal hyperplasia have larger index of positive marcation than in normal areas, inferring that these lesions are associated to AR expression and to the androgenic incentive (Gao et al., 2001).

Huynh et al. (2001) suggest that, in the prostate, the production of specific growth factors such as IGF-I is dependent on androgens. Such factors act in the activation or inhibition of genes that control the cellular cycle, favoring cellular proliferation. Besides, genes that respond to androgens, through AR, are involved in the control of cellular division (Galbraith and Duchesne, 1997). In animals whose cells possess predisposition or alteration genetic, such interaction can aggravate the proliferative character, such as the inductor factor (Pollard and Luckert, 1986). This fact can justify the increase of the AR, mainly in hyperplasic and dysplasic regions of the epithelium.

Zanetoni et al. (2005) showed that the induction of tumor development is highly potentiated in the presence of testosterone in adult gerbils submitted to chemical carcinogenesis. This study points to histopathologic alterations similar to those found in our work such as PIN and adenocarcinomas. Furthermore, the gerbils possess a high index of spontaneous histopathologic alterations during the aging process (Zanetoni and Taboga, 2001), similar to what happens in humans, suggesting the existence of genetic predisposition that can be potentiated after hormonal supplementation. Induction of invasive prostate carcinomas in the rat frequently requires long-term administration of a pharmacological dose of testosterone with or without application of a chemical carcinogen (Shirai et al., 2000).

Franck-Lissbrant et al. (1998) reported that testosterone stimulates angiogenesis in the ventral prostate of mice after castration, possibly from the metabolic necessity of cells after the hormonal incentive. The obtained data suggest apparent increase of the angiogenesis process in the prostate of treated animals, which possibly is involved in the increased energy consumption provoked by the process of cellular synthesis, since the activation of the compound AR-DNA is associated with transcriptional components and coactivators to promote gene transcription (Tsai and O'Malley, 1994).

The prominence of the smooth muscle cells, mainly in pubescent and adult animals, after treatment can be involved with direct anabolic processes, such as cellular hypertrophy and increase of contractile filaments (McArdle et al., 2003). Besides, that fact can be linked to an increase in the synthesis of elements of the extracellular matrix, on account of increase of synthesis organelles including the endoplasmic reticulum, similar to what happens in animals after castration (Vilamaior et al., 2005).

In some areas, the collagen fibers appear in larger amounts in the treated pubescent and adult animals than in the group control, perhaps reflecting a discreet increase in the synthesis of that element of the extracellular matrix. The androgenic receptors are more abundant in the epithelium when compared to the stromal cells (Droller, 1997). Therefore, only an increase in the synthesis of the stromal cells may happen that are responsive to testosterone, causing heterogeneity along the acini in the amount of fibrillar elements.

The decrease in the thickness of the muscular layer in treated aged animals is probably linked to alterations in the synthetic character of SMCs. With the decrease in the testosterone levels, during aging, SMCs start to develop greater synthetic activity, which justifies the increase in collagen fibers and morphologic alterations of these cells (Horsfall et al., 1994; Vilamaior et al., 2005; Pegorin de Campos et al., 2006). With the increase in the testosterone levels, after the treatment, SMCs reestablish a contractile and fusiform character, which promotes a decrease in the

Fig. 14–19. Fig. 14. Ultrastructure figure. Adult treated prostate. Secretory epithelial cells with dilated endomembranes of vesiculous aspect (arrows) for all cytoplasm. Presence of secretion vesicles (sv) and blebs (asterisk). n, nuclei; nu, nucleolus. Scale bar = 1.56 μm. Fig. 15. Ultrastructure figure. Aged treated prostate. Detail of the secretory epithelial cell with prominent Golgi (arrows) and secretion vesicles (asterisk). n, nuclei. Scale bar = 0.56 μm. Fig. 16. Ultrastructure figure. Pubescent treated prostate. Detail of the stroma showing smooth muscle cells with prominent (rer) and evident nucleolus (nu). col, collagen fibers; n, nuclei. Scale bar = 1.56 μm. Fig. 17. Ultrastructure figure. Adult treated prostate. Detail of the stroma showing smooth muscle cells with prominent (rer) and evident nucleolus (nu). col, collagen fibers; n, nuclei. Scale bar = 1.56 μm. Fig. 18. Ultrastructure figure. Aged treated prostate showing the fusiform smooth muscle cells (smc) arrangement in the stroma (st). ep, epithelium. Scale bar = 1.21 μm. Fig. 19. Ultrastructure figure. Aged treated prostate. Subepithelial stroma (st) pointing blood vessels (v) adjacent to the basal laminae (bl). Scale bar = 1.56 μm.

thickness of the muscular layer, similar to that in castrated animals treated with testosterone (Sugimura et al., 1986). Populations of basophilic cells were identified amid the acini epithelium, showing cytoplasmic granular aspect similar to that in neuroendocrine cells described by Capella et al. (1981).

These data demonstrate that the gerbil's prostate is susceptible to androgenic action at the studied ages, showing proliferative and dysplasic effects mainly in adult and aged animals, perhaps suggesting a possible model for the study of induced neoplasias. Besides, they show reversal of some hypertrophic effects of aging mainly on the prostatic stroma, which calls for future studies of this rodent in terms of finding dose-dependent responses with the objective of elucidating the reversibility of aging effects through hormonal therapy.

ACKNOWLEDGMENTS

The authors thank Mr. Luis Roberto Falleiros Júnior and Mrs. Rosana S. Sousa for technical assistance, as well as all other researchers at the Microscopy and Microanalysis Laboratory. This paper is part of the thesis presented by W.R.S. to the Institute of Biology, UNICAMP, in partial fulfillment of the requirement for a PhD degree, and was supported by grants from the Brazilian agencies National Council of Scientific and Technological Development (CNPq; fellowship to W.R.S.).

LITERATURE CITED

Aumüller G, Seitz J. 1990. Protein secretion and secretory process in male accessory sex glands. Int Rev Cytol 121:127–231.

Brandes D. 1966. The fine structure and histochemistry of prostatic glands in relation to sex hormones. Int Rev Cytol 20:207–276.

Buchanan DL, Kurita T, Taylor JA, Lubahn DB, Cunha GR, Cooke PS. 1998. Role of stromal and epithelial estrogen receptors in vaginal epithelial proliferation, stratification, and cornification. Endocrinology 139:4345–4352.

Buchanan DL, Setiawan T, Lubahn DB, Taylor JA, Kurita T, Cunha GR, Cooke PS. 1999. Tissue compartment-specific estrogen receptor-alpha participation in the mouse uterine epithelial secretory response. Endocrinology 140:484–491.

Capella C, Usellini L, Buffa R, Frigerio B, Solcia E. 1981. The endocrine component of prostatic carcinomas, mixed adenocarcinoma-carcinoid tumours and non-tumour prostate: histochemical and ultrastructural identification of the endocrine cells. Histopathology 5:175–192.

Corradi LS, Góes RM, Carvalho, HF, Taboga SR. 2004. Inhibition of 5-alpha-reductase activity induces stromal remodeling and smooth muscle de-differentiation in adult gerbil ventral prostate. Differentiation 72:198–208.

Cotta-Pereira G, Rodrigo FG, David-Ferreira JF. 1976. The use of tannic acid-glutaraldehyde in the study of elastic related fibers. Stain Technol 51:7–11.

Cunha GR, Donjacour AA, Sugimura Y. 1986. Stromal-epithelial interactions and heterogeneity of proliferative activity within the prostate. Biochem Cell Biol 64:608–614.

Custódio AM, Góes RM, Taboga SR. 2004. Acid phosphatase activity in gerbil prostate: comparative study in male and female during postnatal development. Cell Biol Int 28:335–344.

De Carvalho HF, Lino Neto J, Taboga SR. 1994. Microfibrils: neglected components of pressure-bearing tendons. Ann Anat 176:155–159.

Debes JD, Tindall DJ. 2002. The role of androgens and the androgen receptor in prostate cancer. Cancer Lett 187:1–7.

Donjacour AA, Cunha GR. 1993. Assessment of prostatic protein secretion in tissue recombinant made of urogenital sinus mesenchyme and urothelium from normal or androgen-insensitive mice. Endocrinology 131:2342–2350.

Droller MJ. 1997. Medical approaches in the management of prostatic disease. Br J Urol 79(Suppl):42–52.

Franck-Lissbrant I, Häggström S, Damber JE, Bergh A. 1998. Testosterone stimulates angiogenesis and vascular regrowth in the ventral prostate in castrated rats. Endocrinology 139:451–456.

Galbraith SM, Duchesne GM. 1997. Androgens and prostate cancer: biology, pathology and hormonal therapy. Eur J Cancer 33:545–554.

Gao J, Arnold JT, Isaacs JT. 2001. Conversion from a paracrine to an autocrine mechanism of androgen-stimulated growth during malignant transformation of prostatic epithelial cells. Cancer Res 61: 5038–5044.

Góes RM, Zanetoni C, Tomiosso TK, Ribeiro DL, Taboga SR. 2006. Histological response on dorsal and ventral gerbil prostatic lobes induced by different testosterone withdrawal procedures. Micron (in press).

Gömöri G. 1937. Silver impregnation for reticulin in paraffin sections. Am J Pathol 13:993–1002.

Gross AS, Didio LJA. 1987. Comparative morphology of the prostate in adult male and female of Praomys (mastomys) natalensis studies with electron microscopy. J Submicros Cytol 19:77–84.

Hayward SW, Rosen MA, Cunha GR. 1997. Stromal-epithelial interactions in the normal and neoplasic prostate. Br J Urol 79(Suppl 2): 18–26.

Horsfall DJ, Mayne K, Ricciardelli C, Rao M, Skinner JM, Henderson DW, Marshall VR, Tilley WD. 1994. Age-related in guinea pig prostatic stroma. Lab Invest 70:753–763.

Huynh H, Alpert L, Alaoui-Jamali MA, Ng CY, Chan TWM. 2001. Co-administration of finasteride and the pure anti-oestrogen ICI 182,780 act synergistically in modulating the IGF system in rat prostate. J Endocr 171:109–118.

Isaacs JT. 1999. The biology of hormone refractory prostate cancer: why does it develop? Urol Clin North Am 26:263–273.

McArdle W, Katch FI, Katch VL. 2003. Fisiologia do exercício. Rio de Janeiro: Guanabara Koogan.

Mello MLS, Vidal BC. 1980. Práticas de biologia celular. Campinas, Brazil: Edgard Blücher-Funcamp.

Nawa Y, Horii Y, Okada M, Arizono N. 1994. Histochemical and cytochemical characterization of mucosal and connective tissue mast cells of Mongolian gerbil (*Meriones unguiculatus*). Int Arch Allergy Immunol 104:249–254.

Nolan CC, Brown AW, Cavanagh JB. 1990. Regional variations in nerve cell resposnses to the trimethiltin intoxication in Mongolian gerbil. Acta Pathol Microbiol Immunol Scand 81:204–212.

Nomura A, Heilbrun LK, Stemmermann GN, Judd HL. 1988. Prediagnostic serum hormones and the risk of prostate cancer. Cancer Res 48:3515–3517.

Pegorin de Campos SGP, Zanetoni C, Goes RM, Taboga SR. 2006. Biological behaviorof the gerbil ventral prostate in three phases of postnatal development. Anat Rec 288:723–733.

Pinheiro PFF, Almeida CCD, Segatelli, TM, Martinez M, Padovani CR, Martinez FE. 2003. Structure of the pelvic and penile urethra-relationship with the ducts of the sex accessory glands of the Mongolian gerbil (*Meriones unguiculatus*). J Anat 202:431–444.

Pollard M, Luckert PH. 1986. Production of autochthonous prostate cancer in Lobund-Wistar rats by treatments with N-nitroso-N-methylurea and testosterone. J Natl Cancer Inst 77:583–587.

Price D. 1963. Comparative aspects of development and structure in the prostate. Natl Cancer Inst Monogr 12:1–27.

Rosai J. 1996. Male reproductive system. In: Rosai J, editor. Ackerman's surgical pathology, vol. 1, 8th ed. St. Louis: Mosby-Year. p 1221–1256.

Rosner W, Hryb DJ, Khan MS, Nakhla AM, Romas NA. 1999. Sex hormone-binding globulin mediates steroid hormone signal transduction at the plasma membrane. J Steroid Biochem Cell Biol 69:481–485.

Santos FCA, Góes RM, Carvalho HF, Taboga SR. 2003. Structure, histochemistry and ultrastructure of the epithelium and stroma in the gerbil (*Meriones unguiculatus*) female prostate. Tissue Cell 35:447–457.

Santos FC, Leite RP, Custodio AM, Carvalho KB, Monteiro-Leal LH, Santos AB, Góes RM, Carvalho HF, Taboga SR. 2006. Testosterone stimulates growth and secretory activity of the adult female prostate of the gerbil (*Meriones unguiculatus*). Biol Reprod 75:730–739.

Scarano WR, Cordeiro RS, Góes RM, Taboga SR. 2003. Structure and morphometry of pubertal gerbil (*Meriones unguiculatus*) ventral prostate after hormonal therapy. Act Microsc 12:347–348.

Shirai T, Takahashi S, Cui L, Futakuchi M, Kato K, Tamano S, Imaida K. 2000. Experimental prostate carcinogenesis: rodent models. Mutat Res 462:219–226.

So AI, Coll AH, Gleave ME. 2003. Androgens and prostate cancer. World J Urol 21:325–337.

Sugimura Y, Cunha GR, Donjacour AA. 1986. Morphogenesis of ductal networks in the mouse prostate. Biol Reprod 34:961–971.

Taboga SR, Santos AB, Rocha A, Vidal BC, Mello MLS. 2003. Nuclear phenotypes and morphometry of human secretory prostatic cells: a comparative study of benign and malignant lesions in Brazilian patients. Caryologia 56:313–320.

Thomson AA, Foster BA, Cunha GR. 1997. Analyses of growth factor and receptor mRNA levels during development of the rat seminal vesicle and prostate. Development 124:2431–2439.

Thomson AA. 2001. Role of androgens and fibroblast growth factors in prostatic development. Reproduction 121:187–195.

Tsai MJ, O'Malley BW. 1994. Molecular mechanisms of action of steroid/thyroid receptor superfamily members. Annu Rev Biochem 63:451–486.

Vilamaior PSL, Taboga SR, Carvalho HF. 2005. Modulation of smooth muscle cell function: morphological evidence for a contractile to synthetic transition in the rat ventral prostate. Cell Biol Int 29:809–816.

Vilamaior PSL, Taboga SR, Carvalho HF. 2006. Postnatal growth of the ventral prostate in Wistar rats: a stereological and morphometrical study. Anat Rec 288:885–892.

Wang Y, Sudilovsky D, Zhang B, Haughney PC, Rosen MS, Wu DS, Cunha TJ, Dahiya R, Cunha GR, Hayward SW. 2001. A human prostatic epithelial model of hormonal carcinogenesis. Cancer Res 61:6064–6072.

Weibel ER. 1979. Principles and methods for the morphometric study of the lung and other organs. Lab Invest 12:131–155.

Zanetoni C, Taboga SR. 2001. Age-related modifications in stromal and epithelila compartments of the male prostate of *Meriones unguiculatus*. Acta Microsc 3:203–204.

Zanetoni C, Góes RM, Taboga SR. 2005. Experimental induction of prostatic tumors in the gerbil *Meriones unguiculatus*: testosterone effects. Braz J Morphol Sc 22 (Suppl):33–34.